Archives of Toxicology (2022) 96:2447–2464
https://doi.org/10.1007/s00204-022-03314-1

NANOTOXICOLOGY

# Self-regulating novel iron oxide nanoparticle-based magnetic hyperthermia in swine: biocompatibility, biodistribution, and safety assessments

**Sarah Kraus[1] · Ricarina Rabinovitz[1] · Ekaterina Sigalov[1] · Moshe Eltanani[1] · Raz Khandadash[1] · Cheri Tal[1] · Ofra Rivlin[1] · Eddie Sharaga[1] · Pazit Rukenstein[1] · Moshe Cohen-Erner[1] · Abraham Nyska[2] · Yariv Siman-Tov[3] · Ofer Shalev[1]**

Received: 19 December 2021 / Accepted: 11 May 2022 / Published online: 30 May 2022


## Abstracts

Studies demonstrating the successful and safe application of magnetic hyperthermia in large animals are scarce. A therapeutic approach for advanced cancer comprising multicore encapsulated iron oxide (IO) Sarah Nanoparticles (SaNPs), that uniquely self-regulate their temperature, was developed thus overcoming the safety challenges of hyperthermia. SaNPs are intravenously injected and accumulate in tumor tissue, leading to selective heating upon exposure to an external alternating magnetic field (AMF). A series of studies were conducted in healthy swine to assess SaNPs' safety, alone or combined with AMF application. Administration of single high (up to 22 mg IO/kg) or low (3.6 mg IO/kg) SaNP doses had no adverse effects, including no infusion reactions. Vital signs remained stable with no significant clinical pathology changes, and no treatment-associated toxicities. Biodistribution analysis indicated that SaNPs predominantly accumulate in the lungs and clear in a dose- and time-dependent manner. In minipigs that received a single SaNP no-observed-adverse-effect-level (NOAEL)-based dose (3.6 mg IO/kg) with AMF, the average percentage remaining in vital organs after 90 days was 13.7%. No noticeable clinical signs were noted during the 87 to 92-day observation period following irradiation, and no inflammation, necrosis, nor thermal damage were found in the histopathology evaluation. In another minipig, ~ 90 days after three recurrent high doses (14 mg IO/kg), without AMF, almost half of the injected SaNPs were cleared with no residual detrimental effects. We demonstrate that the approach is safe and well tolerated in swine, opening potential avenues as a novel therapeutic modality for cancer patients.

**Keywords** Alternating magnetic field (AMF) · Biodistribution · Complement · Hyperthermia · Magnetic nanoparticles · Safety

## Introduction

Cancer is a major public health problem worldwide and is the second leading cause of death in the United States. The greatest number of deaths are from cancers of the lung, prostate, and colorectum in men and the lung, breast, and colorectum in women (Siegel et al. 2021). Based on projections, cancer deaths will continue to rise with an estimated 11.4 million people dying from cancer in 2030.

The most commonly used treatment modalities for cancer include combinations of surgery, radiation therapy, and chemotherapy that are often associated with the occurrence of adverse effects and long-term sequelae ranging from discomfort-inducing nausea and vomiting to potentially fatal ones such as bone marrow suppression and other immune-related side effects (Nurgali et al. 2018). Novel methods that would minimize side effects while selectively treating cancer, particularly in advanced cases, are needed to aid and enhance standard therapies.

Sarah Nanotechnology is a medical device that comprises Sarah Nanoparticles (SaNPs) and an electromagnetic

✉ Sarah Kraus
sarahk@newphase.co.il

[1] New Phase, Ltd, Odem 5 St, 4934829 Petah Tikva, Israel

[2] Toxicologic Pathology, Sackler Faculty of Medicine, Tel Aviv University, Tel Aviv, Israel

[3] Research and Development Pre-Clinical Department, Shamir Medical Center, Zerifin, Israel

induction system (EIS). The Sarah Nanotechnology approach, named after a patient who succumbed to lung cancer, is aimed primarily for the treatment of stage IV metastatic solid tumors. SaNPs are multicore nanoparticles containing polyethylene glycol (PEG) 20,000-encapsulated iron oxide (IO) clusters, with an average size of 135 ± 25 nm and zeta potential values of (5)-(−30) mV with an average of -(9.7) ± 1.2 mV at neutral pH (Kraus et al. 2021). SaNPs will be intravenously (IV) administered to the patient to preferentially accumulate within tumors via the enhanced permeability and retention (EPR) effect that depends on both the increased leakiness of tumor blood vessels, and the fact that solid tumors lack functional lymphatic drainage, thereby limiting the removal of extravasated nanoparticles from the target site, and leading to prolonged retention within the tumor (Baetke et al. 2015).

Following delivery and accumulation of SaNPs in the malignant tissue, the patient will undergo regional non-ionizing alternating magnetic field (AMF) application with the EIS at a field strength of ~ 8 kA/m and frequency of 290 kHz ± 10%. The SaNPs absorb the electromagnetic energy and convert it to thermal energy, reaching a pre-determined temperature of 50 ± 3 °C, thereby heating the malignant cells and causing hyperthermic cell death at sub-ablative temperatures. To avoid the safety challenges of standard hyperthermia, SaNPs were designed to contain a phase change material (PCM), leading to a unique and inherent ability to regulate their own temperature, thus preventing the occurrence of thermal ablation. The synthesis and characterization of SaNPs are detailed elsewhere (Cohen-Erner et al. 2021).

The PCM has a high energy storage capacity (latent heat), and can absorb, store or release large latent heat over a defined temperature range while the phase change occurs from solid to liquid and vice versa (Sharma et al. 2009). During the phase transition, its capability of absorbing, retaining, and releasing latent heat energy, enables the SaNPs' storage of heat energy and thermal control, thereby preventing overheating of healthy tissue, as opposed to other magnetic IO-based nanoparticles with low control over the heat generation, which limits their therapeutic use to direct administration to target tumor areas and localized heating, or exposure to higher frequency magnetic fields for effective heating (Gneveckow et al. 2004). Magnetic nanoparticles used so far are composed of magnetite ($Fe_3O_4$) and maghemite ($\gamma$-$Fe_2O_3$) IOs, due to their low toxicity and their known metabolic pathways. A magnetic ferrofluid MFL AS, named NanoTherm®, developed by MagForce Nanotechnologies AG, Berlin, Germany has been applied in clinical studies and consists of a core of superparamagnetic IO nanoparticles dispersed in water, coated by an aminosilane type shell, with a diameter of about 15 nm (Thiesen and Jordan 2008). The ferrofluid reacts to the magnetic fields generated by an applicator MFH®300F, developed by the same company, operating at a variable field strength of 0–18 kA/m and frequency of 100 kHz. NanoTherm® therapy has been successfully applied for the focal treatment of tumors, particularly in patients with glioblastoma multiforme and locally recurrent prostate cancer (Maier-Hauff et al. 2007; Johannsen et al. 2010). An additional preparation (RCL-01) containing multicore dextran-coated magnetic IO nanoparticles with a mean particle diameter of 149 nm, has been developed by Resonant Circuits Limited (RCL), London, UK for their use in magnetic field hyperthermia (Tansi et al. 2021). These nanoparticles are directly injected into the tumor followed by AMF application to enhance the therapeutic effect of the standard of care and are currently under clinical testing in patients with locally advanced pancreatic cancer that has not metastasized, as part of the European Commission supported NoCanTher consortium (https://www.nocanther-project-eu).

For their therapeutic effect, SaNPs accumulate in the tumors. However, accumulation in healthy organs is an important risk consideration. Our previous in vivo studies conducted in healthy mice and using a metastatic murine cancer model have shown that SaNPs are safe, biocompatible, and effective when combined with AMF application (Kraus et al. 2021). However, the determination of biocompatibility, biodistribution, and clearance of SaNPs in a larger animal model is essential prior to clinical application to further validate their safety alone and in combination with AMF exposure.

Before initiating human clinical trials, preclinical safety data are needed to ensure the safety of initial clinical doses, the proposed dose escalation, and the duration of clinical dosing in both healthy volunteers and patients. Translation of magnetic hyperthermia to clinical applications has been limited due to the lack of preclinical data on large animals. The relevant animal model of choice should be sensitive enough to unveil all potential toxicities in healthy volunteers and targeted patients. Thus, the selected animal model for preclinical toxicology studies should: (i) have normal health status with a low background incidence of pathological lesions and background diseases; (ii) be amenable to experimental settings; (iii) not be too sensitive to experimental stress; and (iv) be relevant with respect to potential drug-induced adverse effects in humans, including clinical signs of toxicity, clinical pathology, and histopathology (Dixit and Boelsterli 2007).

The use of minipigs as a nonrodent species and as an alternative to dogs and primates is becoming an established model for regulatory toxicity studies designed to assess the safety of new compounds. Moreover, minipigs are the animal model of choice for assessment of drug absorption, tolerance, and systemic toxicity following systemic exposures. Swine are one of the major animal species used in

translational research and preclinical toxicology sharing similar anatomic and physiologic characteristics to those of human beings, particularly in relation to thermo-physiology, such as comparable thermal mass, surface area, water loss through skin, metabolic energy per unit surface area, cardiac output, thermoregulatory mechanisms, and electromagnetic and thermal properties (Swindle et al. 2012), making them clinically relevant and a suitable model for the evaluation of Sarah Nanotechnology, compared with other large animal species. It also provides a highly sensitive and reproducible animal model of complement activation-related pseudoallergy (CARPA) induced by a wide range of nanomedicines. The uniqueness of the porcine CARPA model lies in the close similarities of symptoms to the human CARPA reactions. Several terms are used to describe the CARPA immune reaction, which is acute yet reversible: infusion reaction, anaphylactic/anaphylactoid reaction, or by the name of non-immune allergy. Its symptoms include cardiopulmonary, hemodynamic, clinical pathology, and skin changes that occur within minutes to hours after IV injection of reactogenic nanoparticles. Skin changes are infrequent and variable, arising only in very strong reactions. In some rare cases, CARPA may be life-threatening and even lethal (Urbanics et al. 2015).

The aim of this work was to examine the effects of SaNPs following injection at various doses, either high or low, in the absence or presence of AMF exposure (e.g., full treatment), on potential toxicity and determine their biodistribution and clearance patterns in healthy minipigs as part of the preclinical development process and safety assessment of Sarah Nanotechnology.

## Materials and methods

### Preparation of nanoparticles, dosing, and administration

SaNPs were prepared using the emulsification solvent evaporation method as previously described (Cohen-Erner et al. 2021). Briefly, this preparation method consists in emulsifying an organic phase containing hydrophobic components in an aqueous solution containing Pluronic (PEO – PPO – PEO block copolymer) activated by p-nitrophenyl chloroformate (p-NPC) in dichloromethane, and amine-functionalized 6-arm-branched PEG (Mw = 20 kDa), followed by solvent evaporation and ultrasonication to form an oil-in-water emulsion. Once the residual dichloromethane was evaporated, the SaNP nanoclusters encapsulating IO nanoparticles, PCM, and PEG were formed. The resultant dispersion was thoroughly washed with water and filtered.

For the in vivo studies, sterile SaNPs were used, supplied as a dispersion in water for injection (WFI, B|BRAUN Melsungen AG, Germany) and administered to the animals diluted in 5% glucose, used as vehicle, via an IV infusion into the saphenous vein under control of an infusion pump. Before dilution the SaNPs were sonicated for 6 min in a water bath sonicator at room temperature. An infusion of saline (0.9% sodium chloride), 15–20 mL/kg was administered over ~ 30 min prior to SaNP administration and immediately after completion to keep the animals hydrated.

The dose volumes in the initial studies were determined according to the animals' weight on the day of treatment (10 mL/kg). These doses were relatively high (up to 22 mg IO/kg) and were later on adjusted based on the no-observed-adverse-effect-level (NOAEL) approach that has been employed to identify the highest dose which results in no observed adverse effects (Silva et al. 2021), in accordance to the FDA guideline for the estimation of the maximal safe starting dose in initial clinical trials for therapeutics in adult healthy volunteers (US FDA 2005). The NOAEL is the highest dose tested in an animal species that does not produce adverse effects and corresponds to a clinical SaNP dose, extrapolated from pigs to the human equivalent dose (HED) (US FDA 2005). The first clinical dose to be administered to humans will start at 10% of the 100% HED, after applying the safety factor of 10, according to the FDA guidance.

The initial doses with larger volumes were gradually infused. Approximately 10% of the total volume was first administered over 15 min, followed by 15 min of observation. The remaining dose volume was administered as 2 approximately equal infusions over approximately 1 h each. NOAEL-based doses with smaller volumes were administered as a single infusion at a constant rate of 3 mL/kg/h.

### Animal studies

All studies were reviewed and approved by an Institutional Animal Care and Use Committee (IACUC), followed officially approved procedures for the care and use of animal subjects, and all protocols met the requirements of the local ethical committees of Charles River Laboratories Inc. (OH, USA), under ethical approval numbers CRL-162340-41-42, and Shamir Medical Center (Zerifin, Israel), under ethical approval numbers 14-2019, 35-2019, 25-2020, and 33-2020. All animals were routinely monitored and inspected by a certified veterinarian at the breeding farm, in addition to routine inspections for the purpose of vaccinations and preventive treatments prior to the studies. All animals were also inspected on arrival at the testing facility to verify that they were fit for the study.

A series of experiments were conducted in either Sinclair (Noam Ben Meir, Yokneam, Israel) or Göttingen (Marshall BioResources, North Rose, NY, USA) minipigs, all at the same age of ~ 12 weeks old with a range weight of 9–12 kg and 7–9 kg, respectively. The studies

included the evaluation of sub-acute systemic toxicity and biodistribution of increasing single SaNP doses of 60% (6 mL/kg, 12.6 mg IO/kg) and 80% (8 mL/kg, 15 mg IO/kg) of the maximum dose of 100% (10 mL/kg, 22 mg IO/kg), without or with AMF exposure, and a follow up period of ~ 30 days. Each dose was tested in one animal. The sub-chronic systemic toxicity and biodistribution of repeated SaNP doses of 100% each (14 mg IO/kg), without AMF, were evaluated in one Sinclair minipig that received three IV infusions at an interval of one month between each dosing session with a follow up period of 93 days.

A pre-study examining the acute systemic toxicity and biodistribution in one Sinclair minipig treated with a 156% single NOAEL-based SaNP dose (3.6 mg IO/kg) followed by AMF application with the EIS was conducted before testing the long-term effects of the NOAEL-based SaNP dose in fully treated animals. The selected SaNP dose of 156% represents the maximum dose that a patient would receive in a clinical trial when calculating dose accumulation from repeated dosing, and mimics 3 consecutive doses in human. This animal was followed up for 8 days.

Finally, sub-chronic safety and toxicity were assessed in a study that was carried out in compliance with OECD principles of Good Laboratory Practice (GLP) (Shamir Medical Center, Israel), and comprised of eight Sinclair minipigs (4 males and 4 females) that received a single 156% NOAEL-based dose of SaNP of 3.6 mg IO/kg followed by AMF irradiation at a field strength of 15 mT (12 kA/m) and frequency of 290 kHz ± 10%, compared to control animals (3 males and 3 females) injected with a 5% glucose solution (B|BRAUN Melsungen AG, Germany). The animals were followed up for 87–92 days. All animals were observed daily throughout the acclimation and study courses as detailed below, were fed a commercial swine diet twice a day, and water was provided ad libitum. Animals were fasted overnight prior to sedation and anesthesia. The infusion of the animals tested at Charles River Laboratories (USA) was performed while the animals were fully awake and restrained whereas those tested at Shamir Medical Center (Israel) were dosed under sedation as follows.

For AMF exposure, all animals were sedated with an intramuscular injection of xylazine (2 mg/kg) and ketamine (20 mg/kg). Anesthesia was maintained with inhaled 1–3% isoflurane with supplemental $O_2$. Antibiotic prophylaxis was administered using cefazoline (30 mg/kg). Following experimental procedures, animals were euthanized with a lethal IV injection of potassium chloride solution (B|BRAUN Melsungen AG, Germany), according to the animal facility procedures, and organs were harvested for further analysis.

## AMF exposure

AMF application was conducted using an EIS comprising of 3 main adjunct devices: an electromagnetic induction coil, a radiofrequency (RF) generator, and a chiller that utilizes a closed loop circulating-water system maintained at 15 °C in the coil. Two different preclinical swine systems were used: EIS v.1 model operating at 14 kW (~ 40 kA/m), 225 kHz ± 10% with coil dimensions of 20 × 7 cm (internal diameter x length), manufactured by Braze Solutions LLC, OH, USA, and EIS v.2 model operating at 15 mT (12 kA/m), 290 kHz ± 10% with a larger coil of 20 × 20 cm, manufactured by Ultraflex Technologies, Sofia, Bulgaria.

Studies in the field of hyperthermia have shown that AMF generating systems produce induced electric field within the treated subject. All animal tissues have some degree of electrical conductivity due to their high-water and electrolytes' content. The induced electric field which is generated in the tissue creates eddy currents. The eddy currents running through the resistive tissue result in undesired heating of normal tissues and must be minimized. The magnitude of the eddy currents depends, in part, on the AMF source, frequency and amplitude, and the size of the tissue exposed to the field. One index for measuring AMF exposure dose is the tissue-specific absorption rate (SAR), which is defined as the absorbed electric power per mass in units of W/kg tissue (Nadobny et al. 2015). During AMF exposure, the body surface temperature of the animals was continuously monitored using infrared fiber optic temperature sensors (Optocon, CA, USA). Following anesthetization, the sensors were placed at different positions on the animals' skin, each animal was then wrapped with a circulating-water cooling blanket system (Polar, OH, USA), to prevent body temperature rise during AMF exposure, as such that the area of exposure was completely covered to allow a continuous flow of cold water around it. The animal was then placed in the center of the coil and AMF application commenced 4–8 h post SaNP administration. The AMF body areas of exposure included two different target areas, the thorax or abdomen, in the animals irradiated using EIS v.1 whereas the area of exposure in the animals irradiated using EIS v.2 included a larger area surrounding both the thorax and abdomen. AMF exposure was conducted intermittently for 30 min of three 10 min intervals with ~ 5 min break between each interval.

## Safety endpoints and monitoring of clinical parameters

Morbidity and mortality checks were performed daily. Observations of general clinical signs and symptoms for all animals were conducted before and after treatment, and once a week thereafter. Body weight was measured during acclimation, on the day of treatment, twice a week thereafter,

and prior to termination. Food consumption (binary) was determined based on food completion follow up (normal eating, i.e., food completion/abnormal eating and incompletion of the food) and recorded for all animals daily, from the time of treatment and thereafter. Electrocardiography (ECG) and qualitative assessments for waveform abnormalities were performed in animals that received full treatment sessions before treatment, post injection and after AMF exposure. ECG measurements were collected on unconscious animals with a 12-lead standard (Schiller, AT-101 model). ECG leads were placed at the standard Einthoven positions. Evaluations were performed by a veterinarian.

To measure clinical and hemodynamic parameters, arterial blood pressure, heart rate, oxygen saturation ($SpO_2$), end-tidal carbon dioxide (Et)$CO_2$, and core body temperature were monitored. Arterial blood pressure was measured by placement of a catheter into the femoral artery. The jugular vein was canulated for blood sampling, and the saphenous vein for the administration of SaNP and to maintain a slow and constant drop infusion of either SaNP or 5% glucose (for control animals).

## Blood, urine and coagulation analyses

Blood samples for hematology and clinical chemistry were collected in blood collection tubes (Greiner Bio-One GmbH, Austria) and handled for all animals in all studies at various time points including, baseline (before SaNP administration), post procedure (either SaNP administration or AMF exposure) and on days 2, 3, 4, 7, 14, and 30 (termination day). For the longer studies, time points included $30 \pm 7$ days, $60 \pm 7$ days, and $90 \pm 7$ days. Blood analyses were conducted by the American Medical Laboratories (AML), Ltd., Herzelia, Israel or by Charles River Laboratories Inc. (OH, USA). Collected blood was spun down to separate serum and samples were stored at 4 °C until analysis. The following clinical chemistry parameters were evaluated: alkaline phosphatase, total bilirubin, alanine aminotransferase (ALT), aspartate transaminase (AST), gamma-glutamyl transferase, lactate dehydrogenase (LDH), blood urea nitrogen (BUN), creatinine, creatine phosphokinase (CPK), total protein, albumin, amylase, globulin, albumin/globulin ratio, glucose, total cholesterol, triglycerides, sodium, potassium, chloride, calcium, and phosphorus. Hematology parameters included: white blood cells (WBC), red blood cells (RBC), hemoglobin, hematocrit, mean corpuscular hemoglobin (MCH), mean corpuscular volume (MCV), mean platelet volume (MPV), red cell distribution width (RDW), polymorphonuclear cells, lymphocytes, and platelets counts. Urine analysis and coagulation were evaluated only in the studies in which animals received full treatment sessions with NOAEL-based SaNP doses. Urinalysis included the following: bilirubin, glucose, ketones, pH, protein, specific gravity, RBC, WBC, nitrites, and qualitative urobilinogen. Coagulation parameters included prothrombin time (PT) and partial prothrombin time (PTT). Samples were collected in sodium citrate tubes. Shortly after mixing with anticoagulant, the samples were centrifuged (10 min, 3,000 RPM, 4 °C), the plasma was separated and kept at 4 °C until analyses.

## Necropsy, gross pathology and histopathology

All animals were subjected to a gross necropsy, at termination, which included examination of the external surface of the body, orifices, the cranial, thoracic and abdominal cavities and their contents. Macroscopic findings of all gross lesions in organs were documented. During necropsy, organs (brain, bone and bone marrow, heart, kidneys, liver, mesenteric and sub-mandibular lymph nodes, and spleen), tissues and gross lesions were harvested, wet weighed, and placed in fixative. For the study assessing sub-chronic safety and toxicity conducted under GLP, a full list of collected organs was included as suggested by the international standard for the biological evaluation of medical devices (ISO 10993:11).

Histological slides were prepared by Patho-Lab Diagnostics Ltd., Ness-Ziona, Israel or by Charles River Laboratories Inc. (OH, USA). For the GLP study, the slides were prepared by Alizée Pathology LLC. (MD, USA). Tissues harvested for microscopic examination were fixed in 10% neutral buffered formalin (NBF) for at least 24 h. Tissues were trimmed, according to tissue sampling guides for porcine biomedical models (Albl et al. 2016), embedded in paraffin, sectioned at 5–6 µm, and stained with hematoxylin and eosin (H&E). For the detection of IO nanoparticles, selected tissues were stained with Prussian blue (Frank et al. 2007). Stained slides were examined with an Olympus BX-51 microscope (Olympus, Melville, NY, USA). The evaluation was done in a blinded manner, i.e., without knowing the treatment in each group. Any histopathological findings were recorded, described and scored by a board-certified study Pathologist, using a semi-quantitative scoring system of five grades (0–4), taking into consideration the severity of the changes (0 = No lesion, 1 = Minimal change, 2 = Mild change, 3 = Moderate change, 4 = Marked change) (Schafer et al. 2018).

## Particle electron paramagnetic resonance

SaNP content in tissues was measured using the particle electron paramagnetic resonance (pEPR) method which is based on electron paramagnetic resonance, enabling the direct quantitation of superparamagnetic IO nanoparticles and offering the advantage that there is no need of sample preparation, thereby eliminating manipulation errors and resulting in a higher quality sample set (Gobbo et al. 2015).

The pEPR method, unlike inductively coupled plasma mass spectrometry (ICP-MS) that provides a measure of total sample iron, relies on its ability to distinguish between endogenous (e.g., natural iron molecules present in biological environments) and exogenous iron sources, showing greater selectivity for exogenous magnetic nanoparticles.

For biodistribution evaluation animals were subjected to organ harvesting at their respective scheduled termination. Organ collection included the following: brain, heart, kidneys, liver, lungs, lymph nodes, spleen, all weighed wet as soon as possible following their dissection and individually fixed in pre-labeled tubes containing 10% NBF. All fixed organs were cut into several representative sections using disposable equipment, to avoid cross-contamination. Each section was individually placed in a pre-weighed tube, containing the organ section, and weighed again. The bioanalysis of the samples was performed by Pepric (Leuven, Belgium). To generate a calibration curve, known SaNP dilutions were prepared and measured by pEPR to establish the method's sensitivity and limit of detection (LoD) for each set of samples. Then, all samples were measured and a magnetic signal per volume (µL) was generated for each tube. The signal was then normalized in accordance to the tissue weight in each tube and calculated for each organ sample to obtain the SaNP volume in the whole organ. SaNP percentage in organs was calculated.

### Statistical analysis

All statistical analyses were performed using Graph Pad Prism software (GraphPad Software, La Jolla, CA, USA). Data were analyzed using Student's unpaired *t*-test or one-way analysis of variance (ANOVA), and p-values equal or less than 0.05 were considered statistically significant.

## Results

### Effect of increasing SaNP doses without AMF exposure

In our initial studies, administration of increasing doses of 60% (6 mL/kg, 12.6 mg IO/kg), 80% (8 mL/kg, 15 mg IO/kg), or 100% (10 mL/kg, 22 mg IO/kg) of SaNPs alone without subjection to AMF were first tested in 3 male Sinclair minipigs (Shamir Medical Center, Israel). All animals were followed up for 28–30 days post injection. Prior to SaNP infusion, the animals were sedated and anesthetized followed by endotracheal intubation and catheterization of the femoral artery to measure blood pressure. The introduction of SaNPs and drawing of blood samples were performed via venous catheters. Due to the large volumes of these initial doses, SaNPs were gradually infused. About 10% of the total dose was first introduced followed by two subsequent infusions of the remaining dose volume. The blood pressure, heart rate, respiratory parameters of $SpO_2$ and $EtCO_2$, and body temperature were carefully and continuously recorded before, during and after the entire procedure. All clinical parameters were stable throughout SaNP administration and skin alterations were not observed. Venous thromboembolism (VTE) occurs when a blood clot, or thrombi, forms in a deep vein. Signs of VTE or blocking of blood vessels were not observed during any of the IV SaNP injections conducted in the animals. No mortality occurred throughout the observation periods, all animals gained weight and food consumption was normal.

Blood samples for hematology and clinical chemistry were collected and analyzed throughout the studies at different time points: baseline, 0, 4, 7 h, and on 2, 3, 4, 7, 14, 28, and 30 days after SaNP injection. Clinical pathology parameters remained mostly unaffected and within normal physiologic levels. The main observations are presented in Fig. 1 and included a transient increase at 4 and 7 h post injection in the levels of AST, and alkaline phosphatase, eventually returning to within baseline levels 2–4 days after treatment (Fig. 1A–B). The rise in liver enzymes is likely due to the uptake and subsequent clearance of SaNPs from the liver (Feng et al. 2018). CPK levels were elevated in all animals at 4 and 7 h after the injection and returned to baseline 2–7 days after treatment (Fig. 1C). Fluctuations within normal range in the levels of BUN and creatinine (Fig. 1D) were observed throughout the follow up periods, indicative of normal kidney function. Changes were observed in the LDH levels which increased marginally after the injection, before once again decreasing thereafter (Fig. 1E), without signs of hemolysis or hematocrit changes. LDH catalyzes the conversion of lactate to pyruvate and is not tissue-specific. Therefore, elevated total LDH values may be considered a rather nonspecific finding (Klein et al. 2020).

Most hematology parameters were within reference ranges. An exception in the WBC counts was noted in one pig assigned to the 60% dose (6 mL/kg, 12.6 mg IO/kg) injected group, which decreased on the day of treatment and increased one week after, while in animals treated with higher doses, elevation in WBC counts was noted at 4 h post injection which gradually decreased thereafter (Fig. 1F). The increase in WBC counts was accompanied by a marginal rise in neutrophil counts at 4 and 7 h after the dosing compared to baseline which returned to normal after 4 days (data not shown). Hematological changes of reactogenic nanoparticles in CARPA typically include initial leukopenia followed by protracted leukocytosis and thrombocytopenia: among these the leukopenic effect is the most frequent (Urbanics et al. 2015). Only a single injected pig (60% dose) exhibited low WBC counts, probably reflecting variations between animals and not associated with an infusion reaction.

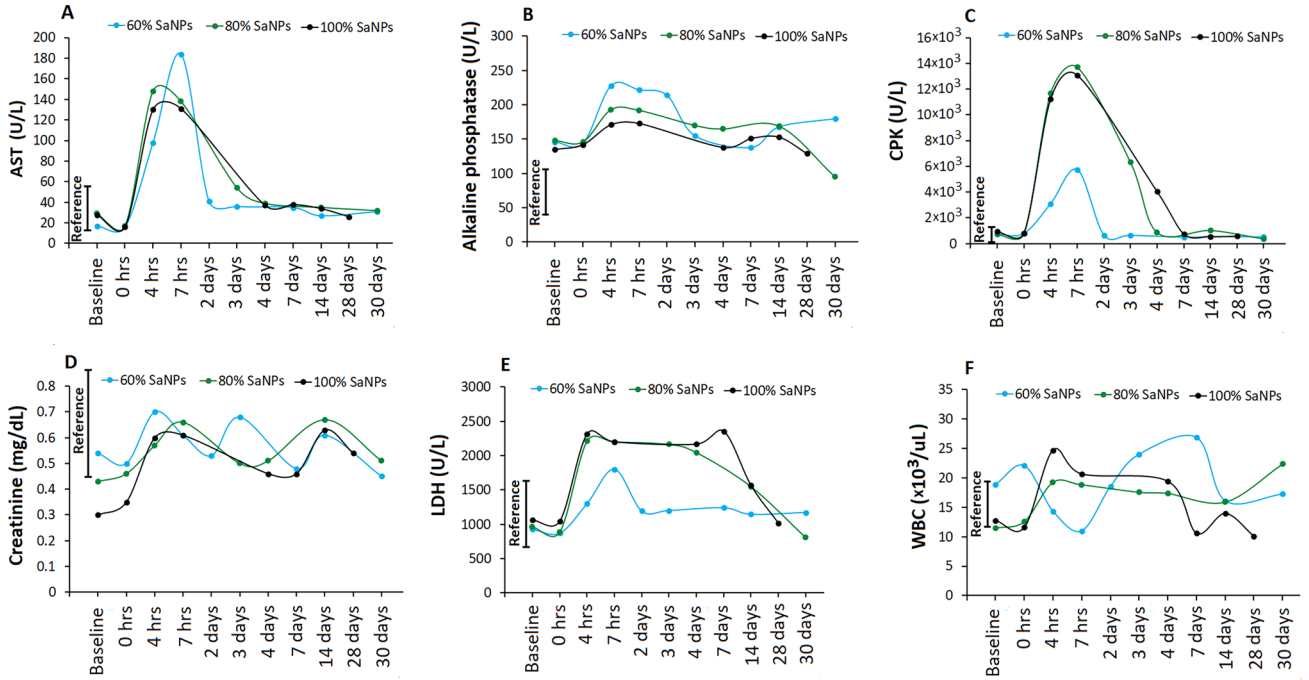


**Fig. 1** Main changes in clinical pathology parameters of animals injected with SaNP doses of 60% (12.6 mg IO/kg), 80% (15 mg IO/kg), and 100% (22 mg IO/kg) over observation periods of ~ 30 days. **A** AST (U/L). **B** Alkaline phosphatase (U/L). **C** CPK (U/L). **D** Serum creatinine (mg/dL). **E** LDH (U/L). **F** WBC ($10^3$/μL) levels. *AST* aspartate transaminase, *CPK* creatine phosphokinase, *IO* iron oxide, *LDH* lactate dehydrogenase, *WBC* white blood cells, *U* units

Histopathology analysis of the brain, bone and bone marrow, heart, kidneys, liver, lungs, mesenteric and sub-mandibular lymph nodes, and spleen revealed no treatment-related toxicity in all animals as no abnormalities were observed upon examination of these organs with the exemption of IO-containing nanoparticles that were identified by Prussian blue staining, showing minimal multifocal positive stained macrophages in the lungs without any inflammation. The pigmented Prussian blue positive granules suggest the presence of SaNP remnants. No such Prussian blue positive granules were noted in any of the other organs examined. Concerning thromboembolism risk, no evidence of thrombosis was observed in the brain, heart, kidneys, liver, and lungs, examined by histopathology. Representative images of the lungs are shown in Fig. 2.

## Effect of single preclinical SaNP doses followed by AMF exposure

The safety of SaNP administration alone set the stage for the next step, examination of the potential toxicity of a single treatment using increasing SaNP doses followed by subjection of different target areas to AMF application. The study included two Göttingen male minipigs that were IV infused with either 60% (12.6 mg IO/kg) or 100% SaNP doses (22 mg IO/kg) (Charles River Laboratories Inc., OH, USA). There were no notable clinical signs during the administration period. Approximately 8 h after the animals were anesthetized and the infusion process was initiated, the AMF was applied to the animals using the EIS v.1 (~ 40 kA/m, 225 kHz ± 10%). Prior to AMF activation, the body surface temperature probes were placed on the animals. The approximate locations of the probes are illustrated in Fig. 3A. The probes were centered under the RF coil of the EIS on the target areas: the thorax in the animal IV injected with a 60% SaNP dose, or the abdomen in the animal IV injected with a 100% dose (Fig. 3B–C). The animals were then wrapped with the cooling blanket system and irradiated in a dorsal position for approximately 15 min, followed by a 5 min break, and then exposure was continued for another ~ 15 min for a total exposure time of 30 min.

There were no abnormal clinical signs related to the AMF exposure noted at the end of the exposure period in any of the animals, which included stable heart rate, blood pressure and respiration parameters. The animals gained weight during the course of the study, there were no intervals of reduced food consumption, and they survived to scheduled euthanasia on day 32.

Changes in hematology parameters were noted in both animals following infusion and prior to AMF exposure, including increased neutrophils and decreased lymphocytes, monocytes, eosinophils, basophils, RBCs, hemoglobin, and

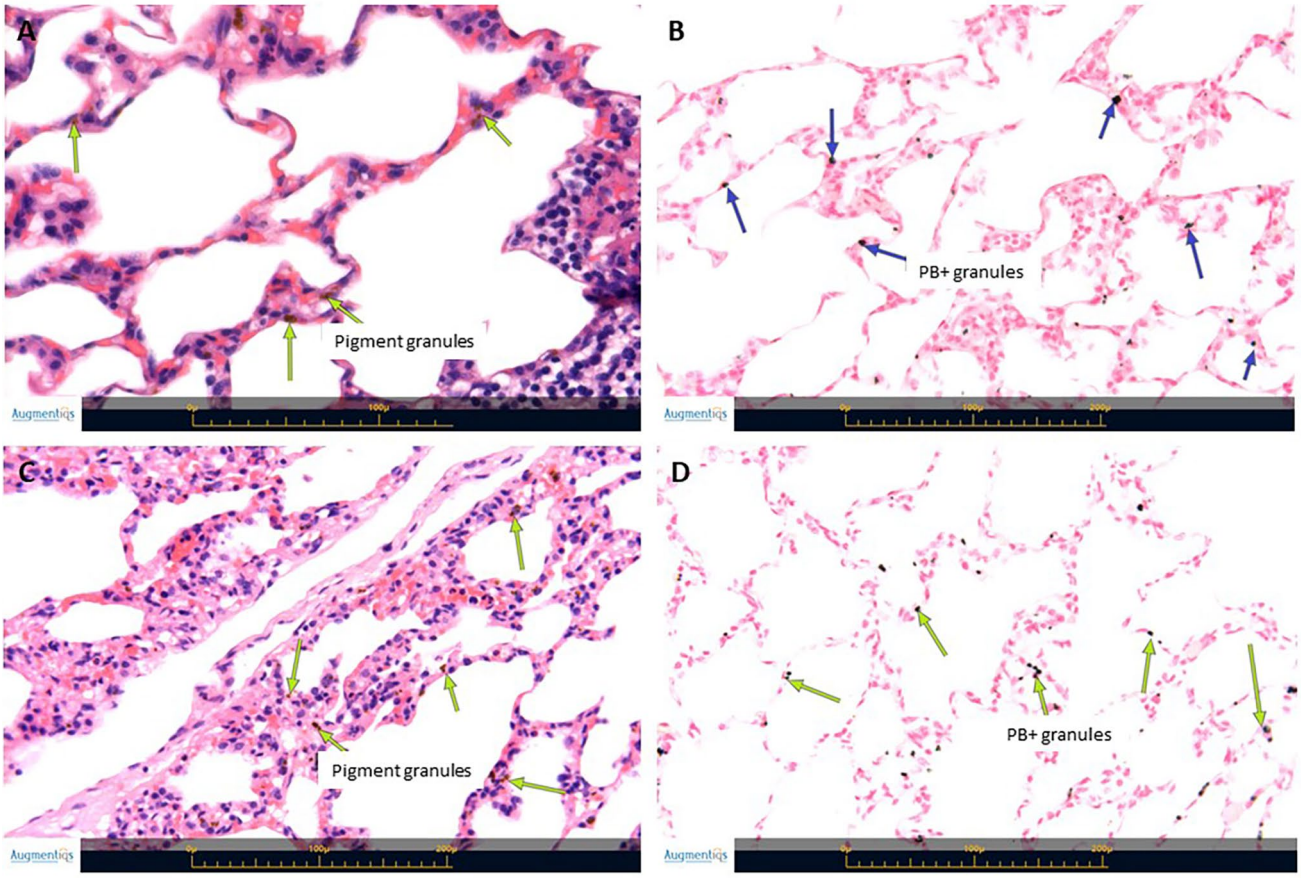


**Fig. 2** Photomicrographs of the lungs of SaNP-infused animals. **A** Lungs section from a pig treated with a single SaNP dose of 80% (15 mg IO/kg) demonstrating multifocal, minimal presence of brownish granules (green arrows) within the interalveolar septa (×60, H&E staining). **B** Prussian blue positive stained granules (blue arrows), suggesting presence of IO (×40). **C** Lungs section from pig treated with a single SaNP dose of 100% (22 mg IO/kg). Green arrows show multifocal, minimal brownish granules within the interalveolar septa (×40, H&E staining). **D** Prussian blue positive stained granules (×40). Images were captured using the Augmentiqs system software (Siegel et al. 2021). *H&E* hematoxylin and eosin, *IO* iron oxide

hematocrit (Fig. 3E). All values were outside of the 95% spread using the historical Charles River Laboratories control data set; however, these changes were transient, generally resolving by day 3 and may have been associated with stress. Stress leukogram is characterized by neutrophilia, an increase in neutrophils, and lymphopenia, a decrease in lymphocytes. Altered levels of circulating leukocytes often reflect a physiologic response to a rise in endogenous glucocorticoid concentrations, such as cortisol, that may occur after a stressful event (Tvedten and Raskin 2012).

In healthy humans, a normal neutrophil to lymphocyte ratio (NLR) is roughly 0.78–3.58 (Forget et al. 2017). NLR serves as a parameter to assess the inflammatory status of a subject and has been proven useful in the stratification of mortality in cardiac events.

In pigs, NLR is considered a reliable stress indicator and has been used to assess physiological stress in commercial growing pigs with values varying with age (Stull et al. 1999). Thus, the mean NLR values in healthy animals at 84 and 112 days of age was found to be ~ 0.8 and similar to humans. On day 1 post injection the NLR was maximal at 7.9, indicative of mild physiological stress. At all other times, the NLR was 1.7 or less, suggesting a lack of physiological stress. Although values remained within normal range, a notable increase in CPK levels was reported following the infusion and before AMF exposure on day 1. CPK values continued to increase through day 3, above the normal range; however, these changes were transient and resolved after one week (Fig. 3D).

There were no significant gross findings observed in any of the animals. The only microscopic change was a minimal amount of pigment in the lung alveolar macrophages with no associated inflammation or tissue response. This finding was also noted in the previous experiment and was consistent with presence of IO derived from the SaNPs by Prussian blue staining.

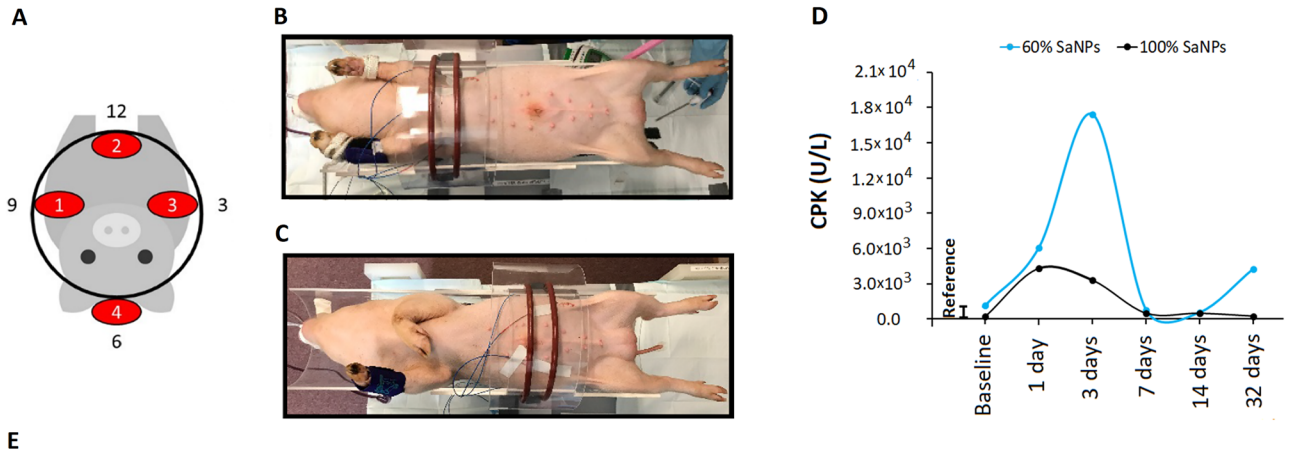


| 60% SaNP dose | | | | | | | | | |
|---|---|---|---|---|---|---|---|---|---|
| Day | WBC 10^3/uL | Neutrophils 10^3/uL | Lymphocytes 10^3/uL | Monocytes 10^3/uL | Eosinophils 10^3/uL | Basophils 10^3/uL | RBC 10^3/uL | Hemoglobin g/dL | Hematocrit % |
| -3 | 11.61 | 5.45 | 5.35 | 0.36 | 0.17 | 0.08 | 8.55 | 13.1 | 40.6 |
| 1 | 11.30 | 9.66 | 1.22 | 0.07 | 0.03 | 0.01 | 6.83 | 10.6 | 33.2 |
| 3 | 8.57 | 3.46 | 4.33 | 0.30 | 0.23 | 0.05 | 8.19 | 12.5 | 39.6 |
| 7 | 7.58 | 2.60 | 4.32 | 0.23 | 0.19 | 0.05 | 8.09 | 12.4 | 39.4 |
| 14 | 10.65 | 3.91 | 6.01 | 0.30 | 0.19 | 0.05 | 8.91 | 13.9 | 46.5 |
| 32 | 8.45 | 3.06 | 4.55 | 0.33 | 0.40 | 0.05 | 9.45 | 14.8 | 45.7 |
| 100% SaNP dose | | | | | | | | | |
| Day | WBC 10^3/uL | Neutrophils 10^3/uL | Lymphocytes 10^3/uL | Monocytes 10^3/uL | Eosinophils 10^3/uL | Basophils 10^3/uL | RBC 10^3/uL | Hemoglobin g/dL | Hematocrit % |
| -3 | 7.27 | 2.02 | 4.76 | 0.23 | 0.11 | 0.02 | 9.14 | 12.6 | 40.5 |
| 1 | 7.22 | 33.7 | 3.15 | 0.20 | 0.04 | 0.01 | 7.63 | 10.8 | 34.4 |
| 3 | 10.09 | 6.06 | 3.51 | 0.13 | 0.14 | 0.11 | 9.02 | 12.7 | 40.4 |
| 7 | 6.74 | 2 | 4.34 | 0.16 | 0.14 | 0.03 | 8.54 | 12 | 38.1 |
| 14 | 7.71 | 2.4 | 4.76 | 0.25 | 0.16 | 0.02 | 9.7 | 13.8 | 45.1 |
| 32 | 7.71 | 2.62 | 4.37 | 0.29 | 0.25 | 0.02 | 10.45 | 14.4 | 46 |

**Fig. 3** Sarah Nanotechnology treatment of Göttingen minipigs exposed to AMF application (EIS v.1, 14 kW, 225 kHz ± 10%) of different target areas following administration of increasing SaNP doses. **A** Approximate locations of temperature sensors. **B** Thoracic area of exposure inside of RF coil (20 × 7 cm) in animal infused with 60% dose (12.6 mg IO/kg). **C** Abdominal area of exposure inside of RF coil in animal infused with 100% dose (22 mg IO/kg). Each animal was irradiated for a total exposure time of 30 min at two intervals of approximately 15 min each. **D** Main changes in hematology parameters throughout the observation period. **E** Changes in CPK values (U/L). *AMF* alternating magnetic field, *CPK* creatine phosphokinase, *EIS* electromagnetic induction system, *IO* iron oxide, *RF* radiofrequency, *U* units

## Effect of repeated SaNP doses without AMF exposure

The purpose of this experiment was to evaluate the subchronic systemic toxicity of repeated SaNP doses of 100% each (14 mg IO/kg), without operating the EIS, in one male Sinclair minipig that received 3 IV infusions at an interval of one month between each dosing session (Shamir Medical Center, Israel). The animal was followed up for 93 days to assess any potential safety issues.

Body weight gain and food consumption were normal throughout the observation period. Clinical parameters recorded during each dosing section showed no significant changes in blood pressure, heart rate, $SpO_2$, $EtCO_2$, body temperature and all values were stable. No significant clinical pathology changes were observed, besides the following minor findings that included, elevated levels of serum creatinine after each dosing session compared to baseline but within normal range, increasing levels of CPK at 7 h after each injection, that returned to normal thereafter, and increasing levels of alkaline phosphatase throughout the study that returned to normal by the end of the study. Other enzymes commonly used as biochemical liver markers such as AST, ALT, and bilirubin remained within normal physiologic levels with some minor fluctuations, supporting normal liver function. WBC counts were elevated at baseline, before SaNP administration, and decreased within normal ranges throughout the study.

Neutrophils behaved similarly with elevated percentages at baseline, and decreasing at day 3 after the first injection. Levels increased at 7 h after each injection and decreased thereafter, within normal ranges, possibly due to neutrophil accumulation around the blood collection cannula. However, no significant nor detectable accumulation around this site was observed microscopically. Furthermore, no evidence of systemic inflammation was observed in any of the organs (liver, lungs, kidneys, brain, and heart) examined by histopathology.

Potential toxicity was also assessed by gross pathology and microscopic examinations of selected organs; brain, spinal cord (cervical, thoracic, lumbar), heart, liver with gallbladder, spleen, lungs, kidneys, bone (femur and sternum) with bone marrow, mandibular and mesenteric lymph nodes, stomach (pyloric, cardiac, fundus), and eyes with optic nerve. The histopathological evaluation demonstrated treatment-related changes in the spleen, liver, and lungs, consisting of minimal (grade 1) presence of pigment within macrophages in these organs. The pigment was confirmed to be positive for Prussian blue stain, consistent with the presence of IO, derived from the SaNPs. Pigment accumulation was not associated with any inflammatory reaction and was therefore not considered as adverse. The cannulated veins were also examined and no signs of inflammation were observed. Representative images of sections taken from the spleen, liver, and lungs are shown in Fig. 4.

## Biodistribution

Biodistribution was determined in selected organs using pEPR analysis. Representative sections from the following organs were measured: liver (left and middle lobes), spleen, lungs (left and right lobes), brain, heart (left ventricular wall, right ventricular wall, interventricular septum, and left atrium), kidneys (left and right), and representative lymph nodes (sub-mandibular, mesenteric). All results were normalized per tissue weight and the individual findings for each organ were expressed as percentage of residual SaNP left in the tissues after the corresponding observation period for each of the animals.

The percentage of total residual SaNP left in the lungs was the highest in all animals compared to other organs, followed by the liver and spleen. There was no residual SaNP or negligible amounts left in the brain, heart, kidneys, and lymph nodes. Therefore, the lungs, liver and spleen were considered to reflect the main accumulation sites in the body. The biodistribution of SaNPs in these organs is shown in Fig. 5A. The total percentage of SaNPs that accumulated in the organs of pigs infused with the higher SaNP doses (12.6–22 mg IO/kg), with or without AMF, is shown in Fig. 5B. The results demonstrated that there was a dose-dependent accumulation and clearance. Clearance of SaNPs from pigs that received 60%, 80%, and 100% doses (12.6, 15 and 22 mg IO/kg), without AMF, was 84.6%, 45.4%, and 38.7%, respectively, after 30 days. For the pigs that received

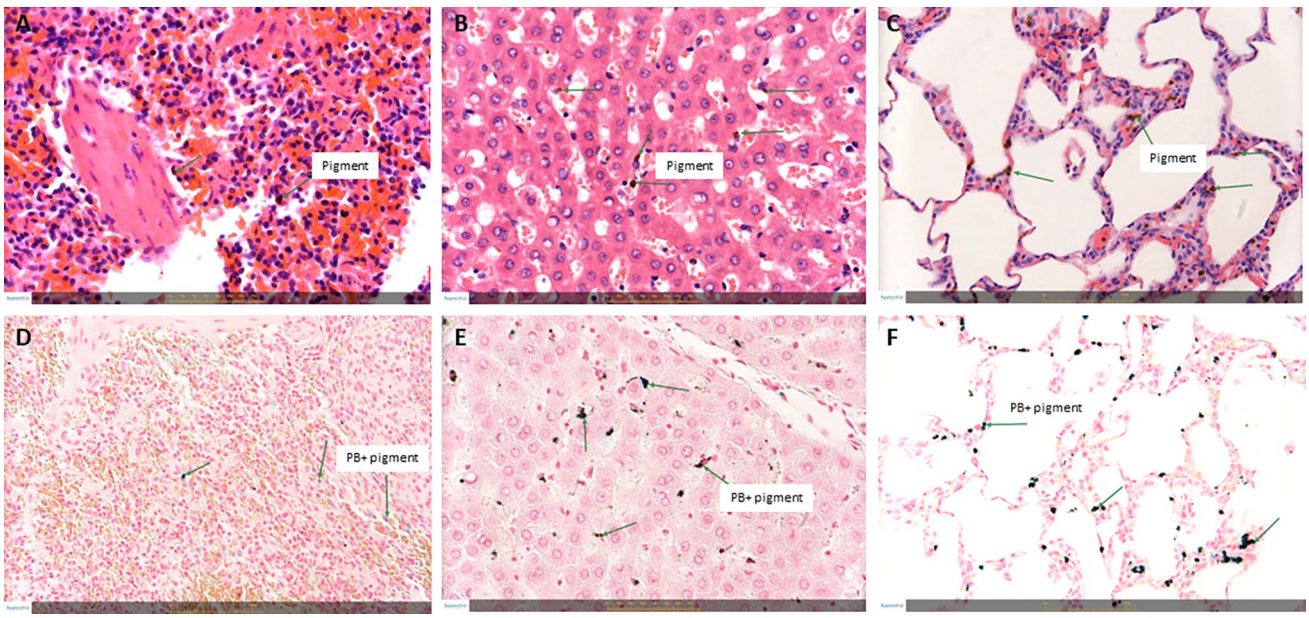


**Fig. 4** Photomicrographs of the spleen, liver, and lungs of an animal infused with 3 repeated SaNP doses of 100% each (14 mg IO/kg). **A** Spleen section (H&E staining). **B** Liver section (H&E staining). **C** Lungs section (H&E staining). Green arrows denote pigment accumulation in these organs. **D** Spleen section (Prussian blue staining). **E** Liver section (Prussian blue staining). **F** Lungs section (Prussian blue staining). Green arrows denote Prussian blue positive stained pigment. Images were captured using the Augmentiqs system software (Siegel et al. 2021). *H&E* hematoxylin and eosin, *IO* iron oxide

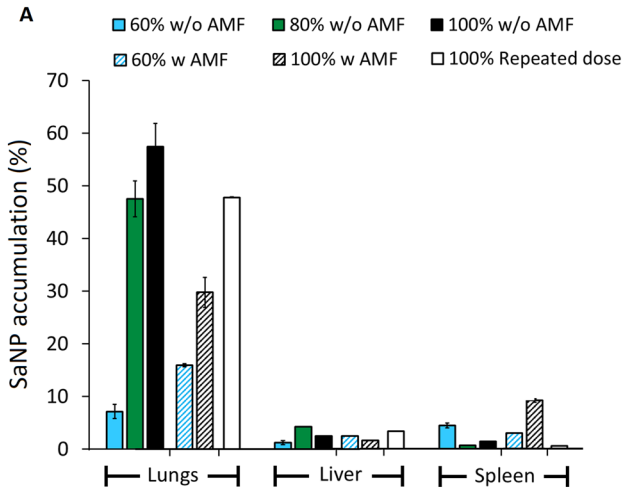


B

| SaNP Dose | AMF | Accumulated | Cleared |
|---|---|---|---|
| 60% | - | 15.4% | 84.6% |
| 80% | | 54.6% | 45.4% |
| 100% | | 61.3% | 38.7% |
| 60% | + | 25.1% | 74.9% |
| 100% | | 41.4% | 58.6% |
| 100% Repeated dose | - | 51.9% | 48.1% |

**Fig. 5** SaNP accumulation and clearance. **A** Percentage of SaNPs accumulated in lungs, liver, and spleen of animals infused with either single (60, 80, 100%) or repeated SaNP doses (100%) with (w) or without (w/o) AMF application. **B** Percentage of total SaNP accumulation and clearance. The animals injected with a single dose were followed up for 30 days, whereas the animal that received repeated doses was observed for 93 days. Biodistribution was determined by pEPR. *AMF* lternating magnetic field, *pEPR* particle electron paramagnetic resonance

60% and 100% (12.6, 22 mg IO/kg) doses followed by AMF application, SaNP clearance was 74.9% and 58.6%, respectively, after 30 days.

Of note, representative urine and feces samples from these animals were collected on day 3 and 30 after SaNP administration to determine the relative excretion of SaNPs through urine and feces. The results were comparative only and showed that while the magnetic signal per volume, determined by the pEPR method, in the urine was close to zero or negligible for both time points, the amount detected in the feces was fivefold higher and decreased with time, suggesting that the SaNPs are mainly eliminated through the feces and not the urine (data not shown).

In the animal that received 3 repeated doses, the total SaNP percentage left in vital organs was 52% which corresponds to 48% SaNP that was cleared from the animal's body after 93 days, showing that the total SaNP percentage left in the vital organs was compatible to the clearance in all animals regardless of AMF exposure. From the

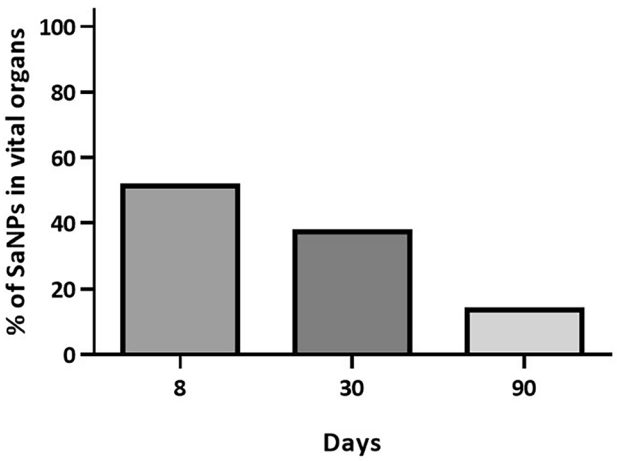


**Fig. 6** Percentage of residual SaNPs left in the lungs, liver, and spleen of animals infused with a single NOAEL-based SaNP dose followed by AMF application. The animals injected with various SaNP doses of 3.32 mg IO/kg, 2.6 mg IO/kg, and 3.6 mg IO/kg were followed up for either 8, 30, or 90 days, respectively. Biodistribution was determined by pEPR. *AMF* alternating magnetic field, *IO* iron oxide, *NOAEL* no-observed-adverse-effect level, *pEPR* particle electron paramagnetic resonance

sub-chronic 90-day study in animals that received a full treatment (SaNP + AMF), two representative animals were evaluated for SaNP biodistribution: one male and one female that received a NOAEL-based dose containing 3.6 mg IO/kg. The analysis of IO content was performed in the liver, lungs, and spleen from these animals, representing the main accumulation sites and thus providing a close estimation of the total amount of residual IO found and cleared from the animals' body after ~ 90 days.

The results showed that the lungs had the highest percentage of residual SaNP, followed by the liver and spleen, in line with our previous data. The percentage of SaNP found in the lungs was $8.2 \pm 2.2\%$ and $7.0 \pm 5.4\%$, in the liver was $4.7 \pm 0.06\%$ and $3.6 \pm 0.02\%$, and in the spleen was $1.5 \pm 1.5\%$ and $2 \pm 0.31\%$, in the male and female pig, respectively. The average total percentage of SaNPs left in these organs at 90 days was 13.7% and similar in both animals, indicating that about 86.3% of the infused SaNPs were cleared from the body after 90 days. The percentage of residual SaNPs left in vital organs of animals followed up for either 8, 30, and 90 days is shown in Fig. 6.

## Acute toxicity evaluation of a NOAEL-based SaNP dose followed by AMF exposure

Before proceeding into examination of the potential toxicity of the full treatment in animals infused with NOAEL-based doses, acute toxicity was evaluated in one animal injected with a single NOAEL-based dose containing 3.32 mg IO/kg followed by AMF application using the EIS v.2 [15 mT

(12 kA/m), 290 kHz ± 10%]. The dose was calculated as described in the Methods section and represents the maximum dose that a patient would receive in a clinical trial when considering dose accumulation from recurrent dosing, and mimics 3 consecutive doses in human, based on the previous biodistribution studies. The fully treated animal was followed up for 8 days to assess any potential safety issues and evaluate the biodistribution of SaNPs.

Clinical parameters recorded during the infusion showed no significant changes in $SpO_2$, $EtCO_2$, and rectal temperature values. An ECG was conducted before and after treatment showing a T wave inversion in all ECG leads, except of aVR and aVL (unipolar limb leads), not associated with any adverse outcome. No significant clinical pathology changes were observed, beside the following findings that included elevated levels of alkaline phosphatase after AMF application that returned to normal on day 8, increased CPK levels following irradiation that remained elevated on day 3 before decreasing once again and returning to normal levels, below the baseline, on day 8. In addition, low yet stable values of serum creatinine were observed. A rise in the percentage of neutrophils, above normal range, accompanied by a minor rise in the WBC count, were noted on the termination day which may have occurred as a result of stress. Since all other immune cell levels were normal and stable, and the NLR value was 2.9 and normal, this finding was not considered to be of clinical significance.

Histopathology evaluation revealed minor changes consisting of minimal presence of pigmented granules, related to the IO-containing SaNPs, within the interstitial and lining alveolar cells in the lungs, and in red pulp macrophages of the spleen that were not associated with any inflammatory reaction. Pigment accumulation within Kupffer cells was found in the liver, associated with minimal (i.e., single cell) hepatocytic necrosis, and minimal presence of neutrophils within the sinusoids (grade 1). As the morphological changes in the liver were of minimal severity, and alkaline phosphatase levels returned to baseline on day 8, they were not considered as adverse according to the criteria of the Society of Toxicologic Pathology (STP) (Kerlin et al. 2016; Palazzi et al. 2016).

The biodistribution analysis showed that after 8 days the percentage of SaNP was the highest in the lungs (45% ± 0.4), followed by the liver (3% ± 0.07), while the percentage of residual SaNPs left in all other organs was under 1%. For example, the concentration in the heart was 0.4% ± 0.02 and in the brain was 0.3% ± 0.005. Negligible amounts were observed in the kidneys (0.2% ± 0.1) and the spleen (0.12% ± 0.001). The amounts in the sub-mandibular lymph node were under the detection threshold (LoD) of the pEPR method and therefore deemed to be 0%. The total percentage of SaNPs found in the pig's organs was 51.3%. Thus, about 49% of the SaNPs were cleared from the body after 8 days, suggesting that half of the SaNPs were cleared during the first week after infusion (Fig. 6).

Based on the results of the observed safety parameters in this animal, including clinical signs, gross pathology, blood analyses, histopathology, and biodistribution the optimal setup conditions for AMF exposure, using EIS v.2 (290 kHz ± 10%), were set to exposure for a total of 30 min of intermittent irradiation (3 intervals of 10 min each with 5 min rest between each interval) at a field strength of 15 mT (12 kA/m).

## Sub-chronic systemic toxicity evaluation of a NOAEL-based SaNP dose and AMF exposure

The full treatment conditions previously established were further validated and assessed for their safety, in a larger group of healthy animals comprising of 4 male and 4 female Sinclair minipigs compared to a control group of 3 males and 3 females infused with vehicle alone (5% glucose solution). The treated animals received a single 156% NOAEL-based dose of SaNP (3.6 mg IO/kg), mimicking 3 consecutive doses in human (to be given once a month for 3 months), followed by AMF exposure with the EIS v.2 [15 mT (12 kA/m), 290 kHz ± 10%] applied at 4 h post the start of infusion, which was between 40 and 58 min, depending on the animals' weight and SaNP concentration (between the range of 1.0–2.5 mg/mL). The target area of exposure included the thorax and abdomen. The temperature sensors were placed on the body surface, each animal was wrapped with the cooling blanket system, in which ~ 15 °C water was circulating, and the irradiation began when the initial mean core temperature of the male and female animals was ~ 34 °C and ~ 33 °C, respectively. Illustrations of a wrapped animal and its positioning inside the coil are shown in Fig. 7A–B. Rectal temperature was measured before AMF exposure, during the breaks and after AMF application. All animals were followed up for 87–92 days and survived to scheduled euthanasia except for one male pig assigned to the treatment group, that was humanely euthanized on day 72 due to illness, confirmed by the study Pathologist to be caused by spontaneous bronchopneumonia and not considered as related to treatment, based on the gross and microscopic findings noted in this single case which are characteristically seen sporadically in untreated pigs. In addition, the lungs' findings were consistent with spontaneous infectious bronchopneumonia which are frequently recorded in pigs and present in this species (Rinke 1997), in particular, the morphological changes were consistent with *Mycoplasma hyopneumoniae* infection (Redondo et al. 2009). However, no samples from this animal were submitted to bacteriological examination.

Similar to the previous experiments, no infusion reactions were observed during SaNP administration and all clinical

A

B

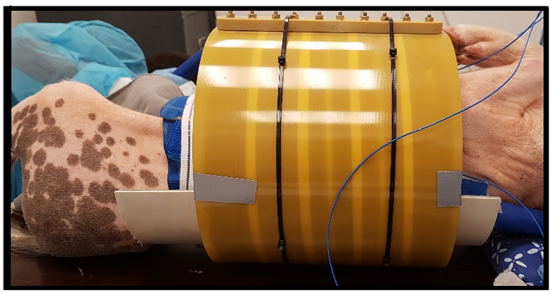

C

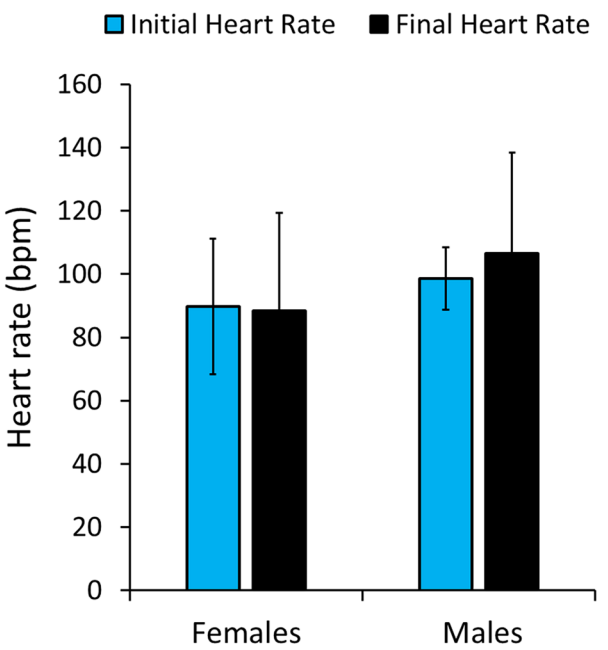


D

| | Animal Weight (kg) | Upper Body Circumference (cm) | Core Temp Start (°C) | Core Temp End (°C)* | Core Temp Rise (°C) | Skin Temp Start (°C) | Skin Temp End (°C)* | Skin Temp Rise (°C) |
|---|---|---|---|---|---|---|---|---|
| Females | 9 | 46 | 31.9 | 30.9 | -1 | 20.83 | 24.7 | 3.87 |
| | 10 | 47.5 | 32.7 | 31.3 | -1.4 | 21.23 | 24.48 | 3.25 |
| | 10 | 50 | 33.6 | 32.3 | -1.3 | 22.65 | 30.05 | 7.4 |
| | 10 | 47 | 32 | 30.6 | -1.4 | 21 | 24.55 | 3.55 |
| **Mean** | **9.75** | **47.63** | **32.55** | **31.28** | **-1.28** | **21.43** | **25.95** | **4.52** |
| **SD** | **0.5** | **1.7** | **0.79** | **0.64** | **0.16** | **0.83** | **2.74** | **1.94** |
| Males | 10 | 49 | 35 | 36.3 | 1.3 | 22.1 | 26.73 | 4.63 |
| | 9.5 | 45.5 | 34.2 | 34.2 | 0 | 20.8 | 23.2 | 2.4 |
| | 10 | 45 | 34.4 | 32.6 | -1.8 | 20.95 | 23.35 | 2.4 |
| | 9.5 | 47 | 34.2 | 28.6 | -5.6 | 24.78 | 29.03 | 4.25 |
| **Mean** | **9.75** | **46.63** | **34.45** | **32.93** | **-1.53** | **22.16** | **25.58** | **3.4** |
| **SD** | **0.29** | **1.8** | **0.38** | **3.26** | **1.84** | **1.84** | **2.82** | **1.19** |

**Fig. 7** Sarah Nanotechnology treatment of Sinclair minipigs exposed to AMF application (EIS v.2, 15 mT, 290 kHz ± 10%) following administration of a single NOAEL-based SaNP dose (3.6 mg IO/kg). **A** Animal wrapped with the cooling blanket system. **B** Animal positioned inside the coil (20 × 20 cm) on a dorsal position. **C** Animals' heart rate (bpm) at the start and end of AMF exposure. **D** Animals' weight, upper body circumference, and changes in mean core and skin temperatures at the start and end of AMF exposure. *AMF* alternating magnetic field, *bpm* beats per minute, *EIS* electromagnetic induction system, *NOAEL* no observed adverse effect level

parameters were stable and normal. All animals showed a healthy appearance and normal activity without lethargy or apathy after treatment and during the follow up period. Body weight gain was normal with no differences in food consumption between the treated and control groups. Clinical pathology changes included an increase in WBC counts above normal reference range, accompanied by increases in neutrophil levels within normal range, in the treatment group immediately after AMF application, probably related to stress leukogram as a result of the SaNP injection or a combination of the injection and the AMF. Changes were transient and levels returned to normal reference range from day 2. An increase in BUN levels in both groups was noted on day 2 compared to baseline results. An increase in blood glucose levels was observed in the two groups immediately after infusion (5% glucose or SaNP) and on day 2, attributed to the presence of glucose in both the vehicle and SaNP preparation. Elevated levels of ALT, AST and

alkaline phosphatase were found in the two groups on day 2 (ALT levels remained high in both groups until day 60). Such an increase is possible when liver enzymes are released into the bloodstream following liver damage. However, no signs of liver damage, which may explain the changes in the enzymes, were observed at necropsy and by the histopathology analyses. Increased CPK levels were noted after AMF application in the treatment group and on day 2 in both groups. Levels were back to normal ranges during the follow up period and increased again on termination day. Clinical pathology, even though some values were higher or lower than the reference values, revealed no adverse effects. This assessment is strengthened due to the fact that similar deviations from normal ranges were observed in the control group's animals as well.

To assess the potential risk of eddy currents' heating in larger tissues, the temperature of the AMF exposed animals was tightly monitored. A rise in body surface and core temperatures is an indication of increased SAR due to eddy currents, and therefore it is important to keep them under control during AMF application to limit the SAR. To minimize the side effects of AMF on normal tissue, the irradiated area of the human body should be limited to a field-frequency product meeting the biological upper limit criterion of $Hf < 5 \times 10^6$ kA/(m s) (Hergt and Dutz 2007), where $H$ denotes the magnetic strength of the applied AMF and $f$ is the frequency. Previous studies in which we aimed to demonstrate the scalability of AMF exposure and evaluate the total power heat that is applied on the thorax and abdomen of a larger animal of 45 kg weight, irradiated at a field strength of 10 mT (8 kA/m) at 300 kHz, as intended in the clinical setting but without SaNP administration, indicated that the frequency to field strength product was $2.4 \times 10^6$ kA/(m s) (8 kA/m at 300 kHz), which was 48% lower than the biological limit (Cohen-Erner et al. 2021). In the current study, all treated animals, exposed to a higher field strength of 15 mT (12 kA/m) had a similar average weight of 9.8 kg and the frequency to field strength product was $3.48 \times 10^6$ kA/(m s) (12 kA/m at 290 kHz), which was still lower than the defined biological limit. The upper body circumference of females and males was $47.63 \pm 1.70$ cm and $46.63 \pm 1.80$ cm, respectively. Since all treated animals had relatively similar body dimensions, particularly those of the target irradiated area, it was assumed that the temperature changes well represented eddy currents. The mean skin temperature of the male animals was 22.16 °C at the start of AMF application and 25.58 °C at the end, resulting in a temperature rise of $3.4 \pm 1.19$ °C. The mean skin temperature of the female animals was 21.43 °C at the start and 25.95 °C at the end of AMF exposure, with a temperature rise of $4.52 \pm 1.94$ °C, slightly higher than the males. All values including initial mean core temperatures at the start and end of the procedure are summarized in Fig. 7D and were $32.55 \pm 0.79$ °C (start) and $31.28 \pm 0.64$ °C (end) in the female and $34.45 \pm 0.38$ °C (start) and $32.28 \pm 093$ °C (end) in the male minipigs. Notably, the cooling of the animals, by the cooling system, was effective in keeping the outer surface (skin) temperature under control.

Examining the effect of AMF application on the heart rate of the animals, the results demonstrated that the heart rate remained relatively stable in female animals (89.75 bpm at start and 88.50 bpm at the end of the exposure) whereas the heart rate in the male animals slightly increased from 98.50 bpm at start to 106.50 bpm at the end of the exposure (Fig. 7C). There were no considerable changes in the heart rates throughout the entire procedure, probably reflecting normal thermoregulatory mechanisms. No abnormal findings were found in the control group animals' ECGs. An inverted T wave was observed post AMF exposure in a single lead, in the treatment group animals' ECG (all males and half of the females). Myocardial ischemia is a common cause of inverted T waves, but are less specific than ST segment depression. In general, an inverted T wave in a single lead in one anatomic segment (i.e., inferior, lateral, or anterior) is unlikely to represent acute pathology. In addition, no signs of cardiac damage, which may explain the changes, were observed at necropsy and by the histopathology analyses and therefore, the inverted T waves observed were of no clinical concern.

The histology and pathology examinations showed no toxic, gross or microscopic treatment-related changes in any of the organs examined which included a full organ list as suggested by the international standard for the biological evaluation of medical devices (ISO 10993:11). In particular, no lesions related to thermal damage were noted in these organs. Studies have shown that nanoparticles are able to cross biological barriers, including those that protect reproductive tissues, and exert toxic effects on organs of the reproductive system. In particular, nanoparticles can pass through the blood–testis barrier, placental barrier, and epithelial barrier, and then accumulate in reproductive organs, thereby inducing organ dysfunction and various adverse effects (Wang et al. 2018). The following reproductive organs were subjected to macroscopic and microscopic evaluation, the prostate, seminal vesicle, testis and epididymis in male animals and the ovaries, vagina and uterus (including cervix and oviducts) in females. Our results demonstrated no toxicity nor pigment accumulation in any of the examined organs.

In all animals from the treated group, minor accumulation of brownish pigment granules was noted within the reticuloendothelial cells located systemically (i.e., liver, lungs, lymph nodes, and spleen) consistent with the previous experiments. The presence of these pigment granules was not associated with any tissue adverse reaction, neither inflammation or necrosis.

## Discussion

This work compiles a series of experiments aimed to assess the biocompatibility and biodistribution of a novel therapeutic approach based on IO nanoparticles and AMF exposure. Our results show that treatment of healthy animals with Sarah Nanotechnology system for safety assessments was well tolerated in two swine models in vivo, both Göttingen and Sinclair minipigs.

Systemic administration of SaNPs at various dose levels, either initial higher doses or lower NOAEL-based, single or repeated doses, with or without AMF application, showed no hemodynamic nor cardiopulmonary alterations in any of the treated animals, as suggested by the clinical and histopathology observations, supporting the absence of cardiovascular distress or infusion reactions, which is critically relevant for safety. A transient but significant rise in the pulmonary arterial pressure is known to be the most prominent and reproducible measure of CARPA in the porcine model, in response to reactogenic nanoparticles. Therefore, pulmonary hypertension is usually quantified as the primary endpoint of hypersensitivity reactions (Szebeni et al. 2018). This symptom is most likely due to the presence of pulmonary intravascular macrophages (PIMs) in the lungs of pigs which can respond to activation by secretion of vasoactive mediators (Urbanics et al. 2015). It should be noted that PIMs are found in several species including pigs, sheep, cattle, horses and cats but not in humans. Although macrophages may accumulate in the intravascular space of the human lung, the underlying mechanism and conditions of PIM cell colonization in this case remain unknown, and it has been suggested that a low percentage of healthy subjects may also host PIM cells in their lungs (Csukás et al. 2015). In consideration that the majority of SaNPs accumulate in the lungs following infusion, and although pulmonary arterial pressure was not measured, all hemodynamic parameters measured (i.e., arterial blood pressure, heart rate, oxygen saturation ($SpO_2$), end-tidal carbon dioxide (Et)$CO_2$, and core body temperature) throughout the IV administration were stable, indicating that no infusion adverse reactions occurred.

It has been proposed that many hypersensitivity reactions to nanoparticles involve complement activation. Depending on their physicochemical properties such as size, morphology and surface patterns, nanoparticles may activate the complement system through the classical, lectin, or alternative pathways (Moghimi and Simberg 2017). In general, nanoparticles induce greater complement activation as their size increase and are also more likely to be internalized by phagocytic cells, due to enhanced opsonization by complement proteins. Moreover, nanoparticles between 40 and 250 nm in size have been shown to induce a potent activation of the complement system through the classical pathway (La-Beck et al. 2021). To examine the ability of SaNPs ($135 \pm 25$ nm) to trigger complement activation, a quantitative assay measuring the levels of the terminal complement complex SC5b-9 was performed in normal human serum, in compliance to GLP regulations, and in sera from lung cancer patients. The results of these studies (data not shown) demonstrated that there was no SaNP-induced complement activation in human samples. Therefore, SaNPs are considered as a 'non-activator of the complement system' (Ekdahl et al. 2018) further supporting the data obtained in our swine studies consistent with the absence of CARPA reactions.

Studies in animal models have described the preferential accumulation of IO nanoparticles in the liver and spleen with few reports also showing the presence of a smaller fraction of the injected IONPs in the lungs (Jain et al. 2008), due to opsonization and subsequent sequestration by the mononuclear phagocyte system (MPS). IO nanoparticles are taken up by the MPS because of their high macrophage content and high level of vascularization and permeability (Arami et al. 2015). Our results demonstrate a dose-dependent accumulation of SaNPs mainly in the lungs, followed by the liver and spleen in swine. Accumulation in these organs was confirmed by extensive histopathology analyses and Prussian blue staining at various time points, showing localization in lung alveolar macrophages, Kupffer cells in the liver, and in splenic red pulp macrophages, without any associated toxicity. The unique lung structure, its large surface area, thin epithelium layer and rich blood supply ensure fast SaNP delivery. In addition, the large accumulation in the lungs might be attributed to the presence of PIMs and uptake of SaNPs by these cells, which are abundantly found in the lungs of pigs (Csukás et al. 2015). PIM cells possess several characteristics that include, ability to adhere to the capillary walls via intercellular adhesion plaques, which secure their stable and lasting direct exposure to the bloodstream, and a ruffled surface that ensures efficient binding and phagocytosis of nanoparticles. PIMs are resident cells in the pulmonary capillaries and represent a part of the MPS in the lungs, similar to Kupffer cells in the liver, whose primary function is the clearance of deleterious agents from the blood, such as bacteria, viruses or nanoparticles that are recognized as foreign materials. Similar biodistribution patterns and dose-dependent accumulation of magnetic nanoparticles in the lungs have been reported in an acute study in pigs, with a final timepoint of 5 h (Edge et al. 2016).

The development of rapidly cleared nanoparticles is an important consideration for biomedical applications and the translation into clinical trials. We hereby demonstrate a time-dependent clearance of almost 90% of the infused SaNPs in swine after 90 days. As suggested by our data, SaNPs are mostly eliminated through the feces.

Histopathological examination of lungs, liver, and spleen samples did not show abnormal changes nor caused long-term changes in enzyme levels suggesting normal organ function. The transient increase in enzymatic activities such as AST, alkaline phosphatase, and CPK in serum of animals upon nanoparticle infusion, at 4 or 8 h post injection, and during the initial days after the injection has been suggested to be a general response of the body and partly the effect of the anesthetic procedure, or saline administration (Thompson et al. 2002; Jain et al. 2008).

Hyperthermia is a promising approach for the application of magnetic nanoparticles for cancer treatment. However, eddy currents are a direct consequence of the applied AMF used to activate the nanoparticles in the tumor and have been shown to limit treatment efficacy in clinical trials. For example, feasibility studies in 22 patients with non-resectable solid tumors treated by thermotherapy using local implantation of a magnetic fluid (MFL AS) consisting of aminosilane coated superparamagnetic IO nanoparticles with a core diameter of 15 nm and IO concentration of 112 mg/mL, in combination with radio- and/or chemotherapy, have shown a slight average elevation by 0.5 °C in body temperatures, an increase in heart rate (average rise of 10 beats/min), and a minor rise of blood pressure in a few patients. Some patients reported local discomfort with tolerance mainly limited by pain in skin folds or at bone surfaces in the pelvic region. In two patients small but superficial burns occurred, resolving under conservative measures and a treatment break of 1–2 weeks (Wust et al. 2006).

An additional prospective phase I study investigating the feasibility of thermotherapy using a similar magnetic fluid consisting of a dispersion of biocompatible magnetic IO nanoparticles, in patients with locally recurrent prostate cancer showed that the median rectal temperature in patients exposed to constant magnetic field strengths between 4 and 5 kA/m (equivalent to 5.0–6.3 mT) was 39.8 °C (38.2–43.4 °C) (Johannsen et al. 2010). Although this study examined local treatment with thermo-ablative temperatures of up to 55 °C in the prostate, no systemic toxicity was observed. In a study examining the efficacy and safety of the Kanzius non-invasive RF hyperthermia system in swine, which operates at a high-power RF of 13.56 MHz, the animals were exposed to repeated RF treatments to the liver. The results indicated negligible treatment-associated toxicities. However, treatment was limited due to fat overheating, measured with fiber optic probes placed into the dermis and subcutaneous tissue overlying the liver (Ho et al. 2017).

Our results in animals exposed to a field strength of 15 mT (12 kA/m) at 290 kHz ± 10% showed low mean core temperatures of ~ 33 °C and ~ 31 °C, in male and female animals respectively, following intermittent AMF application, with an overall temperature decrease from the initial core temperature before irradiation. In addition, an increase in heart rate (average rise of 8 beats/min) was observed in male animals only with no blood pressure changes. The cooling blanket system was effective at controlling the skin and core temperatures and no overheating nor skin burns or thermal damage were observed in any of the organs and/or tissues examined. These results suggest that proper temperature monitoring during AMF exposure can effectively be used as a safety measure. Of note, the optimal irradiation conditions used in our in vivo studies were set to intermittent AMF exposure at 3 intervals of 10 min and are the basis for planned exposure times to be used in the clinical setting. Magnetic hyperthermia using pulse heating has been reported to reduce morbidity due to eddy currents' heating in animals (Ivkov et al. 2005). Moreover, a recent study in mice using pulse sequencing of high-field/low-field sequences, generated by a preclinical system operating at 1.048 ± 0.01 MHz and a magnetic field strength between 4.4 to 8.3 kA/m (equivalent to 5.6–10.5 mT), in a pancreatic cancer model was more effective than a continuous mode in inhibiting tumor growth (Tansi et al. 2021). Although eddy currents are negligible in small animal models, this particular study recommended performing at least two hyperthermia sessions to ensure a maximal impact on tumor reduction.

## Conclusions

The biodistribution of SaNPs plays a key role in defining their therapeutic efficacy and toxicity which are largely dependent on their physicochemical properties. SaNPs' accumulation was observed primarily in the lungs, liver, and spleen with no associated toxicities, when injected alone or following AMF exposure.

Our results indicate that Sarah Nanotechnology treatment was well tolerated in healthy swine without any adverse effects, including infusion reactions, and can therefore potentially be used for safe clinical application. In addition, no abnormalities were noted in the serum biochemical profiles from any of the animals tested, and no pathological lesions were noted on either gross or microscopic examination of tissues. These tests as well as the successful dosing of swine models, at various dose levels, lead to confidence that SaNPs are biocompatible.

SaNP administration followed by AMF exposure produced no detectable toxicity nor tissue injuries, and there was no evidence of any abnormalities or overheating. Our results demonstrate that with proper thermal monitoring, the treatment can be safely applied to pigs. Further thermal modeling is required to predict thermal behavior in humans, overcome potential high SAR issues, and improve patient treatment planning and therapeutic response.

**Acknowledgements** The authors thank Dr Jennifer Fleming, Dr Lynn Lucke, Ms Tal Alon, and Mr Doron Suchi for their valuable comments and fruitful discussions during the studies.

**Author contributions** Conceptualization: SK, OS. Methodology: SK, RK, PR, MC-E. Formal analysis and investigation: SK, RR, ES, ME, ES, AN, YS-T. Writing – original draft preparation: SK, RR. Writing – review and editing: SK, CT, OR, ES, OS. Funding acquisition: OS. Resources: OS. Supervision: SK, OS.

**Funding** This work was supported by New Phase Ltd.

## Declarations

**Conflict of interest** The authors declare the following competing interests: S. Kraus, R. Rabinovitz, E. Sigalov, M. Eltanani, R. Khandadash, C. Tal, O. Rivlin, E. Sharaga, P. Rukenstein, M. Cohen-Erner, O. Shalev are employees at New Phase Ltd. Other authors declare no competing interests.

## References

Albl B, Haesner S, Braun-Reichhart C, Streckel E, Renner S, Seeliger F, Wolf E, Wanke R, Blutke A (2016) Tissue sampling guides for porcine medical models. Toxicol Pathol 44(3):414–420. https://doi.org/10.1177/0192623316631023

Arami H, Khandhar A, Liggitt D, Krishnan KM (2015) In vivo delivery, pharmacokinetics, biodistribution and toxicity of iron oxide nanoparticles. Chem Soc Rev 44(23):8576–8607. https://doi.org/10.1039/c5cs00541h

Baetke SC, Lammers T, Kiessling F (2015) Applications of nanoparticles for diagnosis and therapy of cancer. Br J Radiol 88(1054):20150207. https://doi.org/10.1259/bjr.20150207

Cohen-Erner M, Khandadash R, Hof R, Shalev O, Antebi A, Cyjon A, Nyska A, Goss G, Hilton J, Peer D (2021) $Fe_3O_4$ nanoparticles and paraffin wax as phase change materials embedded in polymer matrixes for temperature-controlled magnetic hyperthermia. ACS Appl Nanomaterials. https://doi.org/10.1021/acsanm.1c02676

Csukás D, Urbanics R, Wéber G, Rosivall L, Szebeni J (2015) Pulmonary intravascular macrophages: prime suspects as cellular mediators of porcine CARPA. Eur J Nanomed 7(1):27–36. https://doi.org/10.1515/ejnm-2015-0008

Dixit R, Boelsterli UA (2007) Healthy animals and animal models of human disease(s) in safety assessment of human pharmaceuticals, including therapeutic antibodies. Drug Discov Today 12(7–8):336–342. https://doi.org/10.1016/j.drudis.2007.02.018

Edge D, Shortt CM, Gobbo OL, Teughels S, Prina-Mello A, Volkov Y, MacEneaney P, Radomski MW, Markos F (2016) Pharmacokinetics and bio-distribution of novel super paramagnetic iron oxide nanoparticles (SPIONs) in the anaesthetized pig. Clin Exp Pharmacol Physiol 43(3):319–326. https://doi.org/10.1111/1440-1681.12533

Ekdahl KN, Persson B, Mohlin C, Sandholm K, Skattum L, Nilsson B (2018) Interpretation of serological complement biomarkers in disease. Front Immunol 9:2237. https://doi.org/10.3389/fimmu.2018.02237

Feng Q, Liu Y, Huang J, Chen K, Huang J, Xiao K (2018) Uptake, distribution, clearance, and toxicity of iron oxide nanoparticles with different sizes and coatings. Sci Rep 8(1):2082. https://doi.org/10.1038/s41598-018-19628-z

Forget P, Khalifa C, Defour JP, Latinne D, Van Pel MC, De Kock M (2017) What is the normal value of the neutrophil-to-lymphocyte ratio? BMC Res Notes 10(1):12. https://doi.org/10.1186/s13104-016-2335-5

Frank JA, Kalish H, Jordan EK, Anderson SA, Pawelczyk E, Arbab AS (2007) Color transformation and fluorescence Prussian blue-positive cells: Implications for histologic verification of cells labeled with superparamagnetic iron oxide nanoparticles. Mol Imaging 6(3):212–218

Gneveckow U, Jordan A, Scholz R, Brüss V, Waldöfner N, Ricke J, Feussner A, Hildebrandt B, Rau B, Wust P (2004) Description and characterization of the novel hyperthermia- and thermoablation- system MFH®300F for clinical magnetic fluid hyperthermia. Med Phys 31(6):1444–1451. https://doi.org/10.1118/1.1748629

Gobbo OL, Wetterling F, Vaes P, Teughels S, Markos F, Edge D, Shortt CM, Crosbie-Staunton K, Radomski MW, Volkov Y, Prina-Mello A (2015) Biodistribution and pharmacokinetic studies of SPION using particle electron paramagnetic resonance, MRI and ICP-MS. Nanomedicine (lond) 10(11):1751–1760. https://doi.org/10.2217/nnm.15.22

Hergt R, Dutz S (2007) Magnetic particle hyperthermia – Biophysical limitations of a visionary tumor therapy. J Mag Mag Mater 311:187–192. https://doi.org/10.1016/j.jmmm.2006.10.1156

Ho JC, Nguyen L, Law JJ, Ware MJ, Keshishian V, Lara NC, Nguyen T, Curley SA, Corr SJ (2017) Non-invasive radiofrequency field treatment to produce hepatic hyperthermia: Efficacy and safety in swine. IEEE J Transl Eng Health Med 5:1500109. https://doi.org/10.1109/JTEHM.2017.2672965

Ivkov R, DeNardo SJ, Daum W, Foreman AR, Goldstein RC, Nemkov VS, DeNardo GL (2005) Application of high amplitude alternating magnetic fields for heat induction of nanoparticles localized in cancer. Clin Cancer Res 11(19 Pt 2):7093s–7103s. https://doi.org/10.1158/1078-0432.CCR-1004-0016

Jain TK, Reddy MK, Morales MA, Leslie-Pelecky DL, Labhasetwar V (2008) Biodistribution, clearance, and biocompatibility of iron oxide magnetic nanoparticles in rats. Mol Pharm 5(2):316–327. https://doi.org/10.1021/mp7001285

Johannsen M, Thiesen B, Wust P, Jordan A (2010) Magnetic nanoparticle hyperthermia for prostate cancer. Int J Hyperthermia 26(8):790–795. https://doi.org/10.3109/02656731003745740

Kerlin R, Bolon B, Burkhardt J et al (2016) Scientific and regulatory policy committee: Recommended ("best") practices for determining, communicating, and using adverse effect data from nonclinical studies. Toxicol Pathol 44(2):147–162. https://doi.org/10.1177/0192623315623265

Klein R, Nagy O, Tóthová C, Chovanová F (2020) Clinical and diagnostic significance of lactate dehydrogenase and its isoenzymes in animals. Vet Med Int 2020:5346483. https://doi.org/10.1155/2020/5346483

Kraus S, Khandadash R, Hof R, Nyska A, Sigalov E, Eltanani M, Rukenstein P, Rabinovitz R, Kassem R, Antebi A, Shalev O, Cohen-Erner M, Goss G, Cyjon A (2021) Novel nanoparticle-based cancer treatment, effectively inhibits lung metastases and improves survival in a murine breast cancer model. Front Oncol 11:761045. https://doi.org/10.3389/fonc.2021.761045

La-Beck NM, Islam MdR, Markiewski MM (2021) Nanoparticle-induced complement activation: Implications for cancer nanomedicine. Front Immunol 11:603039. https://doi.org/10.3389/fimmu.2020.603039

Maier-Hauff K, Rothe R, Scholz R, Gneveckow U, Wust P, Thiesen B, Feussner A, von Deimling A, Waldoefner N, Felix R, Jordan A (2007) Intracranial thermotherapy using magnetic nanoparticles combined with external beam radiotherapy: Results of a feasibility study on patients with glioblastoma multiforme. J Neurooncol 81:53–60. https://doi.org/10.1007/s11060-006-9195-0

Moghimi SM, Simberg D (2017) Complement activation turnover on surfaces of nanoparticles. Nano Today 15:8–10. https://doi.org/10.1016/j.nantod.2017.03.001

Nadobny J, Klopfleisch R, Brinker G, Stoltenburg-Didinger G (2015) Experimental investigation and histopathological identification of acute thermal damage in skeletal porcine muscle in relation to whole-body SAR, maximum temperature, and CEM43°C due to RF irradiation in an MR body coil of birdcage type at 123 MHz. Int J Hyperthermia 31(4):409–420. https://doi.org/10.3109/02656736.2015

Nurgali K, Jagoe RT, Abalo R (2018) Editorial: Adverse effects of cancer chemotherapy: anything new to improve tolerance and reduce sequelae? Front Pharmacol 9:245. https://doi.org/10.3389/fphar.2018.00245

Palazzi X, Burkhardt JE, Caplain H, Dellarco V, Fant P, Foster JR, Francke A, Paul Germann S, Gröters S, Harada T, Harleman J, Inui K, Kaufmann W, Lenz B, Nagai H, Pohlmeyer-Esch G, Schulte A, Skydsgaard M, Tomlinson L, Wood CE, Yoshida M (2016) Characterizing "adversity" of pathology findings in nonclinical toxicity studies: Results from the 4th ESTP International Expert Workshop. Toxicol Pathol 44(6):810–824. https://doi.org/10.1177/0192623316642527

Redondo E, Masot AJ, Fernández A, Gázquez A (2009) Histopathological and immunohistochemical findings in the lungs of pigs infected experimentally with Mycoplasma hyopneumoniae. J Comp Pathol 140(4):260–270. https://doi.org/10.1016/j.jcpa.2008.12.008

Rinke M (1997) How clean is a mini-pig? – Impressions and suggestions of a pathologist working in the field of toxicology. Pharmacol Toxicol 80(Suppl 2):16–22. https://doi.org/10.1111/j.1600-0773.1997.tb01983.x

Schafer KA, Eighmy J, Fikes JD, Halpern WG, Hukkanen RR, Long GG, Meseck EK, Patrick DJ, Thibodeau MS, Wood CE, Francke S (2018) Use of severity grades to characterize histopathologic changes. Toxicol Pathol 46(3):256–265. https://doi.org/10.1177/0192623318761348

Sharma A, Tyagi VV, Chen CR, Buddhi D (2009) Review on thermal energy storage with phase change materials and applications. Renew Sustain Energ Rev 13:318–345. https://doi.org/10.1016/j.rser.2007.10.005

Siegel RL, Miller KD, Fuchs HE (2021) Jemal A (2021) Cancer statistics. CA Cancer J Clin 71(1):7–33. https://doi.org/10.3322/caac.21654

Silva AV, Ringblom J, Moldeus P, Törnqvist E, Öberg M (2021) Benchmark dose-response analyses for multiple endpoints in drug safety evaluation. Toxicol Appl Pharmacol. https://doi.org/10.1016/j.taap.2021.115732

Stull CL, Kachulis CJ, Farley JL, Koenig GJ (1999) The effect of age and teat order on alpha1-acid glycoprotein, neutrophil-to-lymphocyte ratio, cortisol, and average daily gain in commercial growing pigs. J Anim Sci 77(1):70–74. https://doi.org/10.2527/1999.77170x

Swindle MM, Makin A, Herron AJ, Clubb FJ Jr, Frazier KS (2012) Swine as models in biomedical research and toxicology testing. Veterinary Pathol 49(2):344–356. https://doi.org/10.1177/0300985811402846

Szebeni J, Bedőcs P, László D, Urbanics R (2018) A porcine model of complement activation-related pseudoallergy to nano-pharmaceuticals: Pros and cons of translation to a preclinical safety test. Prec Nanomed 1(1):63–73. https://doi.org/10.29016/180427.1

Tansi FL, Maduabuchi WO, Hirsch M, Southern P, Hattersley S, Quaas R, Teichgräber U, Pankhurst QA, Hilger I (2021) Deep-tissue localization of magnetic field hyperthermia using pulse sequencing. Int J Hyperthermia 38(1):743–754. https://doi.org/10.1080/02656736.2021.1912412

Thiesen B, Jordan A (2008) Clinical applications of magnetic nanoparticles for hyperthermia. Int J Hyperth 24(6):467–474. https://doi.org/10.1080/02656730802104757

Thompson JS, Brown SA, Khurdayan V, Zeynalzadedan A, Sullivan PG, Scheff SW (2002) Early effects of tribromoethanol, ketamine/xylazine, pentobarbitol, and isoflurane anesthesia on hepatic and lymphoid tissue in ICR mice. Comp Med 52(1):63–67

Tvedten H, Raskin RE (2012) Leukocyte disorders. Small Animal Clin Diagnosis Laboratory Methods. https://doi.org/10.1016/B978-1-4377-0657-4.00004-1

US FDA (2005) Guidance for industry: Estimating the maximum safe starting dose in initial clinical trials for therapeutics in adult healthy volunteers. Rockville, MD: US Food and Drug Administration

Urbanics R, Bedőcs P, Szebeni J (2015) Lessons learned from the porcine CARPA model: constant and variable responses to different nanomedicines and administration protocols. Eur J Nanomed 7(3):219–231. https://doi.org/10.1515/ejnm-2015-0011

Wang R, Song B, Wu J, Zhang Y, Chen A, Shao L (2018) Potential adverse effects of nanoparticles on the reproductive system. Int J Nanomedicine 13:8487–8506. https://doi.org/10.2147/IJN.S170723

Wust P, Gneveckow U, Johannsen M, Böhmer D, Henkel T, Kahmann F, Sehouli J, Felix R, Ricke J, Jordan A (2006) Magnetic nanoparticles for interstitial thermotherapy – feasibility, tolerance and achieved temperatures. Int J Hyperthermia 22(8):673–685. https://doi.org/10.1080/02656730601106037